J Nanopart Res (2014) 16:2683
DOI 10.1007/s11051-014-2683-9

RESEARCH PAPER

A naked eye aggregation assay for Pb^{2+} detection based on glutathione-coated gold nanostars

Agnese D'Agostino · Angelo Taglietti · Barbara Bassi · Alice Donà · Piersandro Pallavicini

Received: 18 July 2014 / Accepted: 29 September 2014 / Published online: 8 October 2014

Abstract Gold nanostars (AuNS) with a mean hydrodynamic size of 40 nm, obtained with a seed-growth approach using a zwitterionic surfactant (laurylsulfobetaine, LSB), were successfully coated with glutathione (GSH), obtaining a stable and purified solid product which can be easily stored and re-dissolved on need in 0.1 M aqueous solution of Hepes buffered at pH 7. Upon exposure to micromolar concentrations of Pb^{2+} cation, the GSH-coated nano-objects undergo a fast aggregation followed by sedimentation leading to complete precipitation in about an hour. The subsequent disappearing of the intense LSPR extinction can of course be followed spectrophotometrically but, most importantly, can be easily detected with the naked eye. No signs of this event are noticed when other divalent cations are added to the colloidal suspension in the same condition. A careful investigation was performed to study this selectivity and the behaviour of aggregation as a function of time and Pb^{2+} cation concentration. We demonstrate that an easy, rapid, instrument-free, visual detection of micromolar levels of Pb^{2+} is thus possible with this assay, showing a good selectivity towards other investigated metal cations.

Keywords Anisotropic gold nanoparticles · Glutathione · Aggregation · Visual detection · Pb(II) detection · Nanoscale sensor

Introduction

In a classical definition, derived mainly from supramolecular chemistry, a sensory system could be envisaged as a "selectivity + signal" device, in which a receptor unit, selective for a certain analyte, is covalently or coordinatively bound to a signalling unit, able to display a property whose magnitude changes substantially as a result of the interaction of the analyte with the receptor. For example, using as a signalling unit a cromophoric or fluorgenic moiety, the spectral features can be influenced by a binding event with the analyte, which happens in solution. Thus, any change which can be perceived by the naked eye (Fabbrizzi et al. 1995) or with a simple instrument (spectrofluorimeter, Uv–vis spectrophotometer) is particularly precious, leading to quick qualitative determination of the presence of substances of interest, for example pollutants, poisons or biologically relevant molecules (Fabbrizzi et al. 2000; Marcotte and Taglietti 2003).

A completely different approach to colorimetric detection of several kinds of analytes in solution

Electronic supplementary material The online version of this article (doi:10.1007/s11051-014-2683-9) contains supplementary material, which is available to authorized users.

A. D'Agostino · A. Taglietti (✉) · B. Bassi · A. Donà · P. Pallavicini
Dipartimento di Chimica, Università di Pavia, viale Taramelli, 12, 27100 Pavia, Italy
e-mail: angelo.taglietti@unipv.it

comes from exploitation of the plasmonic features of noble metal nanoparticles (Elghanian et al. 1997; Daniel and Astruc 2004; Saha et al. 2012). The use of these kind of devices as probes for visual detection of ions has gained a huge attention in the last years. The development of colorimetric sensing devices based on the variation of LSPR rely usually on aggregation of opportunely functionalized nano-objects induced by binding of an analyte (Hutter and Pileni 2003; Tokareva et al. 2004; Arduini et al. 2005). The position of LSPR bands is sensibly influenced, in addition to several other features like size, shape, nature of the coating agent, solvent and media (Liu et al. 2008), by interparticle distance (El-Sayed 2001; Elghanian et al. 1997), and thus aggregation usually produces a shift in plasmonic peaks, which can be easily measured by means of simple spectrophotometric apparatus, or even clearly perceived with naked eye.

To obtain such kind of simple sensory systems for heavy metal cations, which can be contaminants with serious effects on human health, two features are important: the presence of a robust coating agent on the nano-object surface, to ensure stability and avoid formation of the bulk material even in highly saline media (Amato et al. 2011; Taglietti et al. 2013), and some binding property exerted by the same coating agent, to ensure a specific interaction with the given cation, or at least a good degree of selectivity towards it. Furthermore, this molecule should be able to only partially fill the coordination demand of the cation, causing the cation itself to look for at least two coordinating moieties to complete its coordination sphere. If these conditions are verified, one can expect that the presence of cation in the colloidal suspension of the nano-object will cause cross-linking between them, resulting in an aggregation which could be perceived as a neat colour change of the colloidal suspension.

Following this strategy, several examples have been presented in the recent past, based on spherical Ag and Au nanoparticles coated with different ligands, such oligo–DNA fore Hg^{2+} detection (Lee et al. 2007), histidine-based ligand for Fe^{3+}, (Guan et al. 2008) cysteine for Cu^{2+}, (Yang et al. 2007) just to name a few. One of the most used ligands is glutathione (GSH), which has several features which are strategic for the purpose: in addition to the mercapto function, ensuring a robust binding to noble metal surfaces, GSH has two free-COOH groups and one NH_2 group ready to bind to cations, with an affinity which can be tuned on the basis of the groups protonation and thus as a consequence of pH values (Fu et al. 2012). Quite a lot of aspects have still to be explained on the features of these sensory systems, mainly from the point of view of the reasons of selectivity towards certain cations. Nevertheless, GSH-capped nanospheres have been used for detection of Ni^{2+}, (Fu et al. 2012; Li et al. 2009), As^{3+} (Li et al. 2011) and Pb^{2+} (Beqa et al. 2011; Chai et al. 2010).

Except a few examples, silver and gold nanoparticles used with this approach are of spherical size, even if in the last years some examples of anisotropical noble metal nanoparticles coated with GSH have been reported (Durgadas et al. 2011; Sung et al. 2013).

Among the divalent cations worth of investigations, Pb^{2+} is of particular importance, as it is one of the most toxic for human health. Lead cation can also become a pollutant for drinking water. In the famous "lead in drinking water crisis" in Washington, DC, residents of the District of Columbia were subject to a high rise of lead cation concentration in drinking water, as a consequence of the change of disinfectant from free chlorine to chloramine in November 2000. This altered the water chemistry, causing the leaching of lead cations from lead line pipes and other plumbing materials. In some cases, lead concentration found in samples (taken during the leaching peak in early 2004) exceeded 300 ppb (Guidotti et al. 2009; Edwards et al. 2009). As can be clearly understood, there is a strong and constant need to develop methods able to provide quick, inexpensive and on-site monitoring of lead presence in drinking waters and more generally in environment.

Recently, we have proposed a synthesis of anisotropic gold nanoparticles based on seed-mediated growth approach, using a neutral surfactant, laurylsulphobetaine (LSB). Using this method, a mixture of nano-objects (nanospheres, nanostars and asymmetric nanobranched objects) can be obtained, with a morphology distribution and subsequent extinction spectra with features which can be tuned on the base of synthetic conditions, for example LSB and ascorbic acid concentrations (Casu et al. 2012). In all colloidal suspension obtained, anyway, one can always observe the presence of three plasmonic features, called respectively the short (520–530 nm), intermediate

(600–700 nm) and long (750–1,100 nm) band, which correspond to nanospheres (20 nm diameter), to which the 520–530 nm LSPR band is obviously attributed; nanostars, with large trapezoidal branches (intermediate band); branched asymmetric NPs, with narrow, long branches (long band) of high aspect ratio (AR).

Moreover, we have recently described a procedure to purify Ag nano-objects from unreacted species coming from the synthetic steps, by means of coating nano-objects with a self-assembled monolayer of GSH, which binds to noble metal nanoparticles surface with the sulphur atom of the thiolic function, followed by precipitation at a proper pH and centrifugation, yielding robust, purified AgNP to be used as antibacterial agents (Amato et al. 2011; Taglietti et al. 2013).

On the basis of all these facts, we propose here a simple protocol to obtain purified and robust gold nano-objects coated with GSH, which were then investigated in order to test the ability of the system to act a sensor for Pb^{2+} in solution. It will be demonstrated that a quick and selective visual response caused by aggregation of nano-objects and subsequent precipitation are obtained with micromolar quantities of Pb^{2+}, even in the presence of other divalent cations.

Results and discussion

Coating of AuNS with glutathione

AuNS, synthesized with the seed-growth method that we have recently described (Pallavicini et al. 2011, Casu et al. 2012), are stabilized by the presence of LSB surfactant. After a first centrifugation step in order to remove excess of LSB and other reagents, a proper concentration of GSH (2×10^{-5} M) is added. LSB is thus removed from the nano-objects surface: the thiolic group of GSH easily deprotonates, and sulphur atom can directly bind to gold surface, bringing GSH to substitution of the surfactant molecules (Pallavicini et al. 2011, Casu et al. 2012).

A first indication of this event can be obtained by a simple UV–Vis spectra, as reported in Fig. 1. The spectra of LSB stabilized AuNS are, as expected, composed of three plasmonic bands, reflecting the composition of objects mixture. As synthetic conditions strongly affect the size, shape and populations of objects, it is impossible, even with identical synthetic steps, to obtain identical colloids with identical spectra. For example, repeating identical preparations, long wavelength band ranges between 790 and 850 nm. As a function of this value and of the obtained population of mixture of objects, intermediate band can appear as a proper band or as a shoulder.

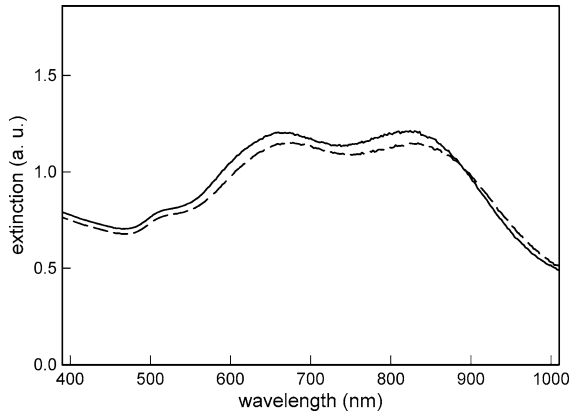

Fig. 1 Representative spectra of a colloidal suspension of AuNS: as prepared, after centrifugation (*solid line*); after GSH addition (*dashed line*)

In all cases, addition of GSH causes a moderate shift (about 8 ± 3 nm) in the LSPR frequencies, a phenomenon which can be explained on the basis of the change of refractive index caused by thiolic coating agent (Pallavicini et al. 2011; Casu et al. 2012).

The GSH-coated AuNS were then characterized by means of DLS measurements. Z-potential at different pH was registered, obtaining a behaviour which is

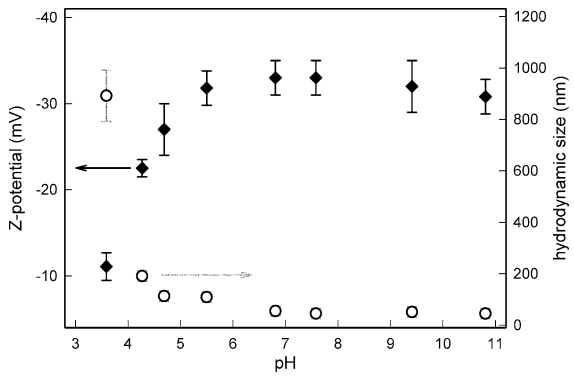

Fig. 2 Z-potential (*black diamond, left axis*) and estimated hydrodynamic size (*white circles, right axis*) of a suspension of AuNS-GSH in water, with varying pH

described in Fig. 2 (black diamonds). As can be clearly observed, at pH higher than 7 the GSH-coated AuNS have a distinctly negative and constant negative z-potential (close to −30 mV), as a consequence of GSH net negative charges caused by the two carboxylate groups which are completely deprotonated. In these conditions, electrostatic repulsion ensures the colloid stability (Amato et al. 2011; Taglietti et al. 2013). On lowering pH, GSH is brought stepwise close to its zwitterionic form, and Z-potential is raised to less negative values. Under pH 4, precipitation of the colloid was visually perceived, and Z-potential was found to reach a value close to −10 mV. Thus, we decided to measure the hydrodynamic size of the objects. As colloidal suspensions here used are polydispersed systems of particles having different shape and size, it is obvious that values obtained from DLS measurement should just be regarded as an indication of the object sizes. Anyway, as can be seen in Fig. 2 (white circles), some interesting information can be obtained: the hydrodynamic size given by the instrument for neutral/basic pH is, as expected (Cavallaro et al. 2013) of about 40 ± 15 nm. When pH is brought under the value of 4.5, a sensible increase of the hydrodynamic size is observed, indicating the formation, at pH lower than 4, of aggregates with dimensions which can reach 1 micron. The precipitation at these pH values is thus explained with the aggregation of the AuNS-GSH, promoted by (i) the reaching of an overall neutral charge around the particles (ii) the electrostatic interactions between the coating layer and in particular to $COO^- \cdots NH_3^+$ bond formation (Amato et al. 2011; Taglietti et al. 2012).

Quick and quantitative precipitation of the colloid can thus be obtained simply reaching pH 3 by adding a few drops of nitric acid to the colloidal suspension after GSH coating.

These data were confirmed by TEM images (see supplementary information): Fig. S1 shows the TEM images obtained on a GSH-coated colloid with pH adjusted to a value of 7. When the measurement is repeated on a colloid which was brought under pH 4 just before deposition on the TEM grid, a marked and quantitative aggregation of nano-objects is observed (S2).

The phenomena can be followed visually: it can be clearly noticed that, on lowering pH the suspension quickly decolours, as formation of large aggregates is expected to produce their fast sedimentation.

Sedimentation or centrifugation of the coated NP solution brought to the appropriate pH value yields stable products, which can be separated and thus purified from reaction mixtures. In this way, AuNS-GSH can be obtained and stored as purified solid products, which can be re-dissolved in water buffered at pH 7 with 0.1 M Hepes.

Behaviour of AuNS-GSH with metal cations: Pb^{2+} detection

Re-dissolution of AuNS-GSH in 0.1 M Hepes at pH 7 gives a colloidal dispersion whose spectra show the expected LSPR bands, with only slight changes as compared to those observed prior to precipitation–purification treatments. The z-potential in these conditions was measured using DLS, giving a value of −25 ± 3 mV.

We also tried to dissolve AuNS-GSH in different solvent systems. Attempts to use PBS buffer were unsuccessful. We noticed that spectrum of AuNS-GSH, immediately after re-dissolution in PBS, was completely different from the spectra obtained for freshly prepared AuNS, for AuNS freshly coated with GSH and for AuNS-GSH in 0.1 M Hepes, which are, on the contrary, very similar. The expected three contributions to LSPR spectra were not present in the case of suspensions in PBS: we observed only wide, unstructured extinction spectra which is typical of aggregated samples, which was followed by a quick, complete sedimentation.

The role of Hepes as stabilizing agent for gold nano-objects is not new to literature (Plascencia-Villa et al. 2013), and indeed Hepes acts as a stabilizer of the reported AuNS colloidal suspensions. Infact, uptake in 0.1 M Hepes at pH 7 of native AuNS (after the standard centrifugation to eliminate reaction mixture and surfactant excess, but in the absence of GSH protection) produced a stable colloid, with no changes in spectrum or any other sign of aggregation, with a striking difference to what is observed with PBS, which once again, in a similar experiment, produces massive aggregation.

We also tried to use non-buffered, bidistilled water, but in this case the spectra obtained for re-dissolved AuNS-GSH were poorly reproducible, as aggregation is strongly influenced by pH of resulting suspension (as seen in Fig. 2, aggregation begins for slightly acidic pH value). The pH value, when not controlled

with a buffer, may vary a lot, as a result of small differences in the experimental setup like pH of water used for re-dissolution, the quantity of acid used for AuNS-GSH precipitation, the care and efficiency in the separation of precipitated AuNS-GSH from surnatant, just to name the more evident. Moreover, as already pointed out (Beqa et al. 2011) control of pH value below 8 is essential to ensure that all $–NH_2$ groups are protonated to $–NH_3^+$, and $–COO^-$ (whose preferences for Pb^{2+} are well known) is the only binding site in capping GSH molecules, in order to minimize interferences from other cations coordination. Moreover, in the absence of a buffer, adjusting pH, after resuspension of AuNS-GSH, to the chosen value of 7 with aliquots of standard acid or base is quite laborious and time consuming, leading sometimes to partial or complete colloid aggregation, and giving once again poorly reproducible samples.

For all these reasons, use of an Hepes solution buffered at pH 7 was the obvious choice: anyway, we are planning further investigations to explain these aspects.

When small aliquots of a stock solution of Pb^{2+} were subsequently added to a sample of the suspensions in 0.1 M Hepes, evident changes in the recorded spectra were noticed (see Fig. 3), suggesting the presence of a quick aggregation increasing with Pb^{2+} concentration. After the titration, the suspension was allowed to stand and in one hour a massive precipitation could be observed visually, with almost complete decolouration: the suspension completely lost its intense, deep blue petroleum colour. We registered the TEM images for a mixture undergoing this quick aggregation. As can be seen in Fig. S3, large aggregates are observed when Pb^{2+} is added to a colloidal suspension in Hepes buffered at pH 7 just before deposition on the TEM grid.

When the experiment was repeated with other bivalent cations, in the case of Ni^{2+}, Cu^{2+} and Co^{2+} negligible changes in spectra were noticed, while in the case of Mn^{2+}, Cd^{2+} and Zn^{2+}, small changes were noticed (see Fig. S4), suggesting a very limited aggregation, in any case not leading to noticeable precipitation in the following hours.

Plot of the normalized extinction taken at the maximum of the long band (ranging between 790 and 850 nm, depending on AuNS preparation used) as a function of added metal cations is shown in Fig. 4, indicating that only Pb^{2+} gives a clear signal of particle aggregation in the investigated concentration range. It has to be stressed the fact that no precipitation was observed for all divalent cations considered: in the considered range, only Pb^{2+} causes massive precipitation of the sample yielding a completely transparent solution in a couple of hours, while in the case of other investigated cations, negligible (Cu^{2+}, Ni^{2+} and Co^{2+}) or very limited (Zn^{2+}, Mn^{2+} and Cd^{2+}) changes in the LSPR spectra indicating aggregation are observed.

Noteworthy, when aliquots of Pb^{2+} were added to a colloidal suspension obtained dissolving native AuNS

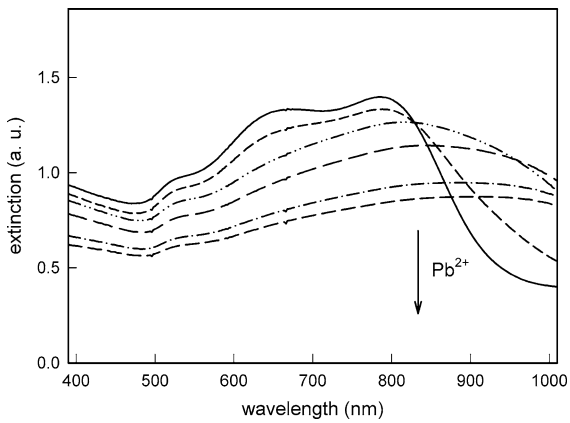

Fig. 3 Spectra of AuNS-GSH colloidal suspension (buffered to pH 7 with 0.1 M Hepes) before (*full line*) and after addition of increasing quantities of Pb^{2+} (from 1 to 5 μM final concentration)

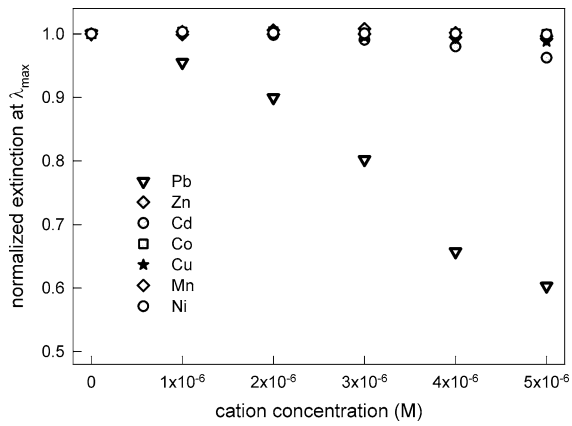

Fig. 4 Plot of the normalized extinction of LSPR band (taken at the maximum of the long band, range 790–850 nm) for a AuNS-GSH colloidal suspension (buffered to pH 7 with 0.1 M Hepes) as a function of the concentration of M^{2+} in the suspension

(after a preliminary centrifugation to eliminate excess surfactants and reactants, but without GSH coating) in 0.1 M Hepes at pH 7, no changes in AuNS spectrum or other aggregation signs were observed, demonstrating that GSH coating is the responsible of the reported aggregation upon cation addition.

We then decided to follow the time evolution of AuNS-GSH colloidal suspension after the addition of fixed quantities of divalent metal cations. In order to do this, to identical samples of colloidal suspension of AuNS-GSH buffered at pH 7 in 0.1 M Hepes, stock solutions of cations were added to give a metal concentration of 3 μM, and spectra evolution were followed. In Fig. S5, the spectra evolution with time after Pb^{2+} addition is shown, while in Fig. S6, as a representative example, the spectra evolution after Cd^{2+} addition is presented. Once again, spectra showed that at this concentration, and in the time range investigated (30 min) quantitative aggregation is observed only in the case of Pb^{2+} addition. Plot of the normalized extinction value at the wavelength of LSPR maximum (measured before adding cation, for this whole set of preparation it was 850 nm) versus time for the experiments on all the cations investigated is given in Fig. 5 as can be clearly observed, addition of Pb^{2+} gives an instantaneous decrease in the absorbance of the long LSPR band, indicating an aggregation, which proceeds with time, while very small effects are registered for other cations.

Thus, at micromolar concentrations, only the presence of Pb^{2+} can be perceived instrumentally

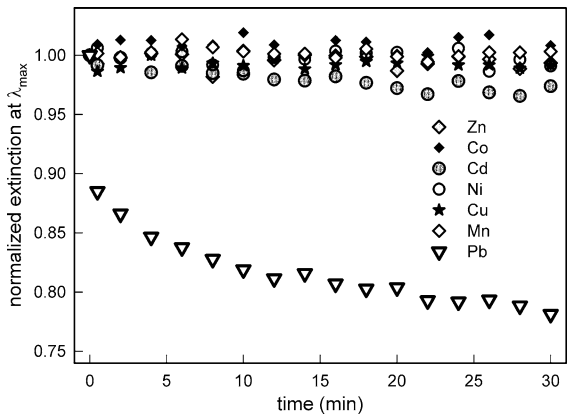

Fig. 5 Normalized extinction for the long band (850 nm) as a function of time, after addition of M^{2+} to a AuNS-GSH colloidal suspension (buffered to pH 7 with 0.1 M Hepes) at 3 μM concentration

but, more importantly, also with naked eye, as a consequence of the strong decolouration of the colloidal suspension. Aggregation and subsequent precipitation are clearly visible as a neat decolouration in the time scale of less than one hour only in the case of Pb^{2+} addition: all other cations investigated do not give any visual response, and negligible instrumental signals, of their presence in solution in the investigated concentration range.

It is worth of citation that in a precedent work (Chai et al. 2010) a similar system based on 5–8 nm diameter spherical gold nanoparticles coated with GSH was used to detect Pb^{2+} in a similar fashion, exploiting spectral changes of colloids upon aggregation. The main differences with this work are the following: (i) in the cited work pH of colloidal suspension was neither controlled with a buffer nor adjusted; (ii) the presence of a certain amount of NaCl is necessary to promote sensible and quick aggregation and colour changes; (iii) no quick and quantitative precipitation is observed, if not in the presence of high quantities (100 micromolar) of Pb^{2+}. For what concerns the two last points, we believe that the different behaviour is mainly due to differences in nanoparticles size and shape, which influence their surface area and subsequently the number of GSH molecules on the objects, which are responsible of the cross-linking between objects themselves as a result of Pb^{2+} complexation, and which causes the aggregation of the colloid. AuNS described here have a mean size of 40 nm and branched shapes, resulting in strong increase of the particle surface area and of number of GSH molecules per object, and thus producing larger aggregations upon Pb^{2+} cation complexation, when compared to smaller spherical nanoparticles used in the cited work.

As experiments described are showing the highest affinity for Pb^{2+} cation, we were interested to evaluate selectivity and competition towards other investigated divalent cations. To a sample of Hepes-buffered AuNS-GSH colloid, we added a stock solution containing Ni^{2+}, Cu^{2+}, Co^{2+}, Mn^{2+}, Cd^{2+} and Zn^{2+}, in order to obtain, in the colloidal suspension, a 3-μM concentration for each metal cation, with an overall M^{2+} concentration of 18 μM. Spectra (see Fig. S7) of colloidal suspension were only slightly altered after addition of the "competing" cations, and, more importantly, precipitation was not observed, even after several (>12) hours. The same experiment was

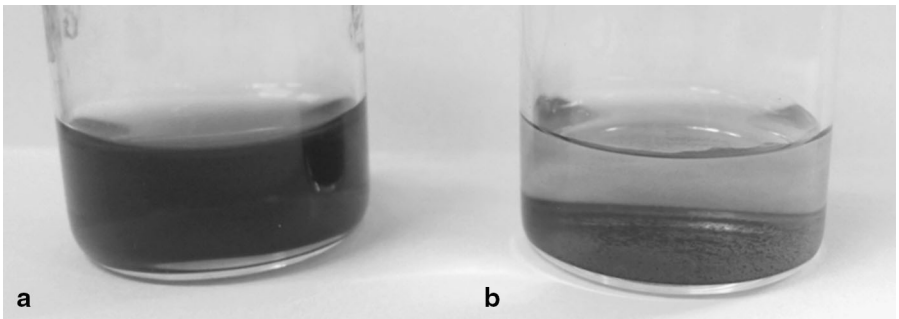

Fig. 6 Photograph of the AuNS-GSH colloidal suspension (in Hepes 0.1 M at pH 7) one hour after: **a** the addition of Ni^{2+}, Cu^{2+}, Co^{2+}, Mn^{2+}, Cd^{2+} and Zn^{2+}, 3 μM each, overall M^{2+} concentration of 18 μM; **b** the same M^{2+} concentration, but in the presence also of 3 μM Pb^{2+}

repeated adding Pb^{2+} to the cation mixture, in order to obtain a final concentration of 3 μM of Pb^{2+} (corresponding to 240 ppb) and an overall 21 μM in divalent cations. In this case, a fast aggregation, identical to the one registered in the presence of 3 μM Pb^{2+} only (in the absence of any interfering cation, as described in Fig. S5) followed by quantitative precipitation in about one hour, as can be clearly seen in Fig. 6, was observed. The same behaviour was observed when repeating the experiment on two samples of AuNS-GSH prepared dissolving solid AuNS-GSH in pure water and then carefully adjusting the resulting suspensions to pH 7 with aliquots of standard acid and base.

Also, Z-potential was measured immediately after the addition of the divalent cation mixture (3 μM in each divalent cation) to the suspensions in Hepes, in the absence and presence of Pb^{2+}, giving, respectively, values of -26 ± 5 and -23 ± 5 mV, values which are almost identical to the one observed for AuNS-GSH objects in the same pH conditions but in the absence of metal cations. In this way, we can rule out the idea that aggregation has to be related to a sensible variation in z-potential caused by cation complexation (which could reduce the overall charge given by carboxylic and ammonium functions).

We also performed an experiment adding different quantities of Pb^{2+} ions to identical samples of a colloidal suspension in Hepes of AuNS-GSH made 18 μM in divalent cations mix (3 μM each one). In order to try to minimize the effect of sedimentation and precipitation, which of course tends to grow with time, for each sample we performed spectra immediately after Pb^{2+} addition: spectra are shown in Fig. 7.

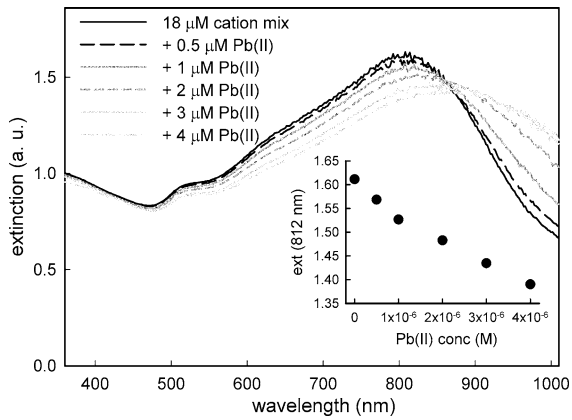

Fig. 7 Spectra of AuNS-GSH colloidal suspension (buffered to pH 7 with 0.1 Hepes) after addition of: *i* a cation mixture (see *text*) to give an overall M^{2+} concentration of 18 μM (*solid black line*); *ii* 18 μM cation mix + increasing quantities of Pb^{2+} (see *legend*). *Inset* plot of absorbance for higher wavelength LSPR maximum (812 nm) as a function of Pb^{2+} concentration in the suspension

It was observed that aggregation-induced decrease of the LSPR maximum has a linear dependence from lead concentration, even in the presence of competing cations (see inset of Fig. 7). As can be seen, variations in LSPR bands which can be related to Pb^{2+}-induced aggregation are obtained as a function of Pb^{2+} added, and a small spectral change can be observed even with submicromolar concentration (0.5 μM of Pb^{2+}, corresponding to 40 ppb) in the presence of quite higher concentration of other cations (overall 18 μM in M^{2+}). Quite interestingly, even for the case of the minimum added Pb^{2+} concentration (0.5 μM), precipitation of the colloidal suspension was observed after a few

hours: in principle, Pb^{2+} presence in quantities lower than 50 ppb can be detected even in solutions containing distinctly higher quantities of other divalent cations.

As already pointed out, (Chai et al. 2010) explanation of this preference towards Pb^{2+} cations is not straightforward: coordination of Pb^{2+} to binding functions of GSH is probably the most favourable in the pH conditions chosen for the assay. It has to be noticed that recently it was demonstrated that gold spherical nanoparticles coated with GSH show selectivity towards metal cations which changes as a function of pH (Fu et al. 2012). Moreover, Hepes complexation of some of the investigated cations (such as Cu^{2+}) cannot be completely excluded (Sokolowska and Bal 2005) and could play a role in complex formation equilibria. Anyway, the experimental results give evidence of the fact that, in the described conditions, only Pb^{2+} is able to give a quantitative cross-linking of the AuNS-GSH objects leading to massive, visible aggregation and precipitation.

At this point, we decided to investigate the aggregation event caused by Pb^{2+} cations with DLS measurements of the hydrodynamic size of dispersed particles. As previously described, the colloidal dispersions used are polydispersed systems of particles with different shape and size, thus the reported values must be regarded as an indication of the mean object sizes, but once again some precious information can be obtained. Typically, DLS measurement on a AuNS-GSH colloid buffered at pH 7 with Hepes, gave a value of about 40 ± 15 nm. The influence of increase in Pb^{2+} concentrations on aggregates formation rate was first measured. In this case, the mean hydrodynamic diameter of the dispersed colloidal particles was measured immediately after the addition of a certain amount of Pb^{2+} and after a lapse of 5 min. As can be seen from Fig. S8, when Pb^{2+} concentration is higher than 1 μM, aggregates are produced immediately, and also evolution to bigger aggregates get faster as concentration increases: with a 5-μM concentration, aggregates bigger than 1 micron grow instantly, explaining the complete precipitation occurring in a short time.

On the other side, in a sample which was made 0.5 μM in Pb^{2+}, hydrodynamic size was determined as a function of time, observing a continuous increase of this value, as shown in Fig. 8. Aggregation in these conditions seems to proceed quite slowly, but is able to produce, in a few hours, objects with a size which can undergo sedimentation and precipitation, as we visually perceived.

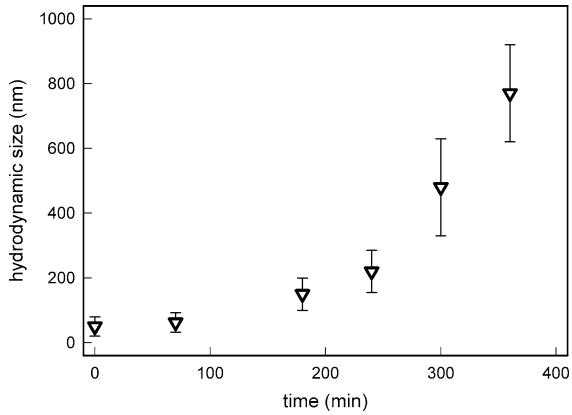

Fig. 8 Hydrodynamic size obtained from DLS measurements, as a function of time, of an AuNS-GSH suspension (buffered to pH 7 with 0.1 M Hepes) after addition of Pb^{2+} 0.5 μM

Conclusions

We have developed a method for coating AuNS with GSH, and this allowed to obtain robustly coated anisotropic gold nano-objects, which can be easily purified from synthetic residual and surfactants, easily stored as a stable solid and re-dissolved on need in Hepes-buffered solution. We demonstrated that these AuNS-GSH, when dissolved in 0.1 M Hepes buffer, offer a simple visual assay for micromolar Pb^{2+} detection at pH 7, based on their fast aggregation to micron-sized objects which quickly give sedimentation, giving a neat decolouration of the blue-coloured colloidal AuNS-GSH suspension. These phenomena can easily be detected with the naked eye, or followed with a simple UV–Vis spectrophotometer. The aggregation is not showed in the presence of all the other heavy metal cations investigated (Ni^{2+}, Cu^{2+}, Co^{2+}, Mn^{2+}, Cd^{2+} and Zn^{2+}), while is caused by sub micromolar Pb^{2+} concentration even in the presence of much higher concentration of the cited divalent cations which were considered as representative of possible interferents. This selectivity and the behaviour of aggregation as a function of time and of Pb^{2+} concentration, were assessed with careful investigations using mainly UV–Vis Spectrophotometry and

DLS measurements. Further studies are in progress to fully understand the mechanism of selectivity and applicability to real biological and environmental samples.

Experimental

Materials and methods

Lauryl sulfobetaine, $HAuCl_4$ (>99 %), L-ascorbic acid (AA), silver nitrate (>99.8 %), sodium borohydride (>99.8 %), L-glutatione reduced (>99 %), Hepes, $Cu(CF_3SO_3)_2$, $Cd(CF_3SO_3)_2$, $Ni(CF_3SO_3)_2$, $Co(CF_3SO_3)_2$, $Zn(CF_3SO_3)_2$, $Mn(CF_3SO_3)_2$ and $Pb(NO_3)_2$ were purchased from Sigma–Aldrich. Reagents were used as received. Glass cuvettes were standard optical glass cuvettes purchased from Hellma. Water was bidistilled, prepared from deionized samples. Glassware materials were carefully cleaned with aqua regia, and then washed several times with bidistilled water under sonication before use.

Synthesis of AuNS with the seed-mediated growth method

Seeds: The seed solution is prepared in a 20 mL vial by mixing 5.0 mL of a 0.20 M LSB solution in water and 5 mL of a 5×10^{-4} M $HAuCl_4$ solution in water. The resulting solution shows a pale yellow colour typical of diluted $AuCl_4^-$. Then an ice cooled solution of $NaBH_4$ 0.01 M (0.600 mL) in water is added. The vial is hand-shaken for 10 s, and the solution assumes the typical brown–orange colour of Au nano seeds.

Growth solution: This is prepared in a 20-mL vial by using LSB solution 0.20 M (5.0 mL) in water and $AgNO_3$ 0.004 M (0.180 mL) in water. To this solution, aqueous $HAuCl_4$ 0.001 M (5.0 mL) is added, thus obtaining a pale yellow colour after gentle mixing. A volume of 0.0788 M aqueous Ascorbic acid solution (0.085 mL) is then added. The solution became colourless after a few seconds of gentle mixing. Then aqueous solution of seed (0.012 mL) is added to solution and the vial is gently hand-shaken for few seconds. Immediately a grey–blue colour appears. Evolution to the final product is fast, and no further colour or spectroscopic changes can be observed after 40 min.

Preparation, purification and re-dissolution of AuNS-GSH

Typically, a sample of AuNS (10 mL) was centrifugated for 13 min at 13,000 rpm. Then the surnatant (colourless) was discarded, and the nano-objects pellet was completely re-dissolved in bidistilled water (10.0 mL). GSH-coated AuNS suspension was prepared by adding GSH solution 0.001 M (0.250 mL) in water to the AuNS colloidal suspensions and leaving the suspension standing for 1 h. Then the sample was acidified with standard HNO_3 solution 0.01 M in water to a pH value of about 3, in order to obtain precipitation of the GSH-capped AuNS. After centrifugation for 5 min at 5,000 rpm and subsequent removal of the surnatant, the nano-objects were stored in glass vials. For further experiments, the stored AuNS-GSH were dissolved typically in 10 mL of 0.1 M Hepes buffer solution adjusted at pH 7, or in pure water, which was then adjusted to pH 7 with small aliquots of standard acid and base solutions.

Behaviour of AuNS-GSH with metal cations

Titration of 10 mL of colloidal suspension of AuNS-GSH, prepared as previously described, was performed adding increasing quantities of a stock solution of divalent cations. In a typical experiment, UV–Vis spectra for the colloidal suspension in the absence of added cation were registered, and then one spectrum was taken 10 s after every addition.

For the mixed cations containing stock solutions, a first one, without Pb^{2+}, was prepared containing a total concentration of metal cations of 0.001 M (1.6×10^{-4} M for each cation). The second one, containing also Pb^{2+}, was once again prepared containing the same total concentration of metals (1.4×10^{-4} M for each cation).

For time-related measurement, after taking a spectrum in the absence of cations, to 10 mL of colloidal suspension of AuNS-GSH, prepared as previously described, for each metal cation investigated a proper quantity of a stock solution was added, in order to have a final concentration of 3 μM. A spectrum was taken 30 s after mixing, then a second one after 90 s. After these first spectra, all the following spectra were taken every 2 min.

All UV–Vis absorbance spectra of colloidal suspensions were taken with a Varian Cary 50

spectrophotometer in the range between 300 and 1,100 nm, using a standard quartz cuvette with 1 cm optical path.

Transmission electron microscopy

Transmission electron microscopy (TEM) images were obtained on colloidal suspensions of AuNS-GSH adjusted at pH 3 and 7 in water soon after GSH addition, and on AuNS-GSH re-dissolved in 0.1 M Hepes at pH 7, after addition of Pb^{2+} ions at final concentration of 5 μM. All samples for TEM were prepared as described and immediately diluted 1:10 with bidistilled water, and soon deposited on Nickel grids (300 mesh) covered with a Parlodion membrane and observed with a Jeol JEM-1200 EX II instrument, using a voltage of 80 kV.

Dynamic light scattering measurements

The dynamic light scattering (DLS) measurements were performed with a *Zetasizer Nano-ZS90* (source: polarized He–Ne laser, 30 mW output power, vertically polarized).

In particular, hydrodynamic size and Zeta potenzial measurements of GSH-AuNS at different pH values were estimated on eight samples of colloidal suspension brought at different pH values. To obtain the chosen pH value (ranging from 3.7 to 11), small quantities of standard solution of HNO_3 0.01 M or NaOH 0.05 M were added. Both measurements of hydrodynamic size and Zeta potential were replicated three times for each pH value.

DLS was also used to measure changes in GSH-AuNS hydrodynamic size in the presence of Pb^{2+}. These measurements were performed on 10 mL of colloidal suspension. To this samples, 0.005 mL of 10^{-3} M $PbNO_3$ 10^{-3} M in water was added, to obtain a Pb^{2+} concentration of 0.5 μM. Immediately after addition (time zero), hydrodynamic measurements were registered. Then, on the same sample, hydrodynamic size of AuNS-GSH was recorded at different fixed time. Hydrodynamic size measurements were replicated three times for each established time.

The influence of the increase in Pb^{2+} concentrations on aggregates formation rate was measured on four samples of AuNS-GSH colloidal suspension (10 ml buffered to pH 7 with 0.1 M Hepes) using DLS. The hydrodynamic diameter of colloidal particles was measured immediately after the addition of a certain amount of lead of a solution of $PbNO_3$ 10^{-3} M in water, in order to have a final concentration in each sample, respectively, of 5×10^{-7} M, 10^{-6} M, 3×10^{-6} M and 5×10^{-6} M. After a lapse of five minutes from the addition of lead solution, hydrodynamic measurements were recorded again on each sample. The measurements were replicated three times for each concentration and established time.

Acknowledgments Funding had been granted by Fondazione Cariplo (Bandi Ricerca Scientifica e Tecnologica sui Materiali Avanzati, 2010-0454), the Ministero dell'Istruzione, Università e Ricerca (MIUR). Authors also want to thank Vittorio Necchi and Centro Grandi Strumenti, for TEM images.

References

Amato E, Diaz-Fernandez YA, Taglietti A, Pallavicini P, Pasotti L, Cucca L, Milanese C, Grisoli P, Dacarro C, Fernandez-Hechavarria JM et al (2011) Synthesis, characterization and antibacterial activity against gram positive and gram negative bacteria of biomimetically coated silver nanoparticles. Langmuir 27(15):9165–9173

Arduini A, Demuru D, Pochini A, Secchi A (2005) Recognition of quaternary ammonium cations by calix 4 arene derivatives supported on gold nanoparticles. Chem Commun 5:645–647

Beqa L, Singh AK, Khan SA, Senapati D, Arumugam SR, Ray PC (2011) Gold nanoparticle-based simple colorimetric and ultrasensitive dynamic light scattering assay for the selective detection of Pb(II) from paints, plastics, and water samples. Acs Appl Mater Interfaces 3(3):668–673

Casu A, Cabrini E, Dona A, Falqui A, Diaz-Fernandez Y, Milanese C, Taglietti A, Pallavicini P (2012) Controlled synthesis of gold nanostars by using a Zwitterionic surfactant. Chem A Eur J 18(30):9381–9390

Cavallaro G, Triolo D, Licciardi M, Giammona G, Chirico G, Sironi L, Dacarro G, Dona A, Milanese C, Pallavicini P (2013) Amphiphilic copolymers based on poly (hydroxyethyl)-D, L-aspartamide : a suitable functional coating for biocompatible gold nanostars. Biomacromolecules 14(12): 4260–4270

Chai F, Wang CA, Wang TT, Li L, Su ZM (2010) Colorimetric detection of Pb^{2+} using glutathione functionalized gold nanoparticles. Acs Appl Mater Interfaces 2(5):1466–1470

Daniel MC, Astruc D (2004) Gold nanoparticles: Assembly, supramolecular chemistry, quantum-size-related properties, and applications toward biology, catalysis, and nanotechnology. Chem Rev 104(1):293–346

Durgadas CV, Lakshmi VN, Sharma CP, Sreenivasan K (2011) Sensing of lead ions using glutathione mediated end to end assembled gold nanorod chains. Sens Actuators B Chem 156(2):791–797

Edwards M, Triantafyllidou S, Best D (2009) Elevated blood lead in young children due to lead-contaminated drinking

water: Washington, DC, 2001–2004. Environ Sci Technol 43(5):1618–1623

Elghanian R, Storhoff JJ, Mucic RC, Letsinger RL, Mirkin CA (1997) Selective colorimetric detection of polynucleotides based on the distance-dependent optical properties of gold nanoparticles. Science 277(5329):1078–1081

El-Sayed MA (2001) Some interesting properties of metals confined in time and nanometer space of different shapes. Acc Chem Res 34(4):257–264

Fabbrizzi L, Pallavicini P, Parodi L, Perotti A, Taglietti A (1995) Molecular recognition of the imidazolo residue by a dicopper(II) complex with a bisdien macrocycle bearing 2 pendant arms. J Chem Soc Chem Commun 23:2439–2440

Fabbrizzi L, Licchelli M, Rabaioli G, Taglietti A (2000) The design of luminescent sensors for anions and ionisable analytes. Coord Chem Rev 205:85–108

Fu R, Li J, Yang W (2012) Aggregation of glutathione-functionalized Au nanoparticles induced by Ni^{2+} ions. J Nanopart Res 14:929

Guan J, Jiang L, Li J, Yang W (2008) pH-dependent aggregation of histidine-functionalized Au nanoparticles induced by Fe^{3+} ions. J of Phys Chem C 112(9):3267–3271

Guidotti TL, Calhoun T, Davies-Cole JO, Knuckles ME, Stokes L, Glymph C, Lum G, Moses, Goldsmith DF, Ragain L (2009) Elevated lead in drinking water in Washington, DC, 2003-2004: The public health response (vol 115, pg 695, 2007). Environ Health Perspect 117(8):A342–A342

Hutter E, Pileni MP (2003) Detection of DNA hybridization by gold nanoparticle enhanced transmission surface plasmon resonance spectroscopy. J Phys Chem B 107(27):6497–6499

Kim YJ, Johnson RC, Hupp JT (2001) Gold nanoparticle-based sensing of "spectroscopically silent" heavy metal ions. Nano Lett 1(4):165–167

Lee J-S, Han MS, Mirkin CA (2007) Colorimetric detection of mercuric ion (Hg^{2+}) in aqueous media using DNA-functionalized gold nanoparticles. Angew Chem Int Edition 46(22):4093–4096

Li H, Cui Z, Han C (2009) Glutathione-stabilized silver nanoparticles as colorimetric sensor for Ni(2 +) ion. Sens Actuators B Chem 143(1):87–92

Li JL, Chen LX, Lou TT, Wang YQ (2011) Highly sensitive SERS detection of As3 + ions in aqueous media using glutathione functionalized silver nanoparticles. Acs Appl Mater Interfaces 3(10):3936–3941

Liu C-W, Huang C-C, Chang H-T (2008) Control over surface DNA density on gold nanoparticles allows selective and sensitive detection of mercury(II). Langmuir 24(15): 8346–8350

Marcotte N, Taglietti A (2003) Transition-metal-based chemosensing ensembles: ATP sensing in physiological conditions. Supramol Chem 15(7–8):617–625

Pallavicini P, Chirico G, Collini M, Dacarro G, Dona A, D'Alfonso L, Falqui A, Diaz-Fernandez Y, Freddi S, Garofalo B et al (2011) Synthesis of branched Au nanoparticles with tunable near-infrared LSPR using a zwitterionic surfactant. Chem Commun 47(4):1315–1317

Plascencia-Villa G, Bahena D, Rodriguez AR, Ponce A, Jose-Yacaman M (2013) Advanced microscopy of star-shaped gold nanoparticles and their adsorption-uptake by macrophages. Metallomics 5(3):242–250

Saha K, Agasti SS, Kim C, Li XN, Rotello VM (2012) Gold nanoparticles in chemical and biological sensing. Chem Rev 112(5):2739–2779

Sokolowska M, Bal W (2005) Cu(II) complexation by "non-coordinating" N-2-hydroxyethylpiperazine-N'-2-ethanesulfonic acid (Hepes buffer). J Inorg Biochem 99(8): 1653–1660

Sung HK, Oh SY, Park C, Kim Y (2013) Colorimetric detection of Co^{2+} ion using silver nanoparticles with spherical, plate, and rod shapes. Langmuir 29(28):8978–8982

Taglietti A, Fernandez YAD, Cucca L, Dacarro G, Grisoli P, Necchi V, Pallavicini P, Pasotti L, Patrini M (2012) Antibacterial activity of glutathione-coated silver nanoparticles against gram positive and gram negative bacteria. Langmuir 28:8140–8148

Taglietti A, Fernandez YAD, Galinetto P, Grisoli P, Milanese C, Pallavicini P (2013) Mixing thiols on the surface of silver nanoparticles: preserving antibacterial properties while introducing SERS activity. J Nanoparticle Res 15(11):1–13

Tokareva I, Minko S, Fendler JH, Hutter E (2004) Nanosensors based on responsive polymer brushes and gold nanoparticle enhanced transmission surface plasmon resonance spectroscopy. J Am Chem Soc 126(49):15950–15951

Yang WR, Gooding JJ, He ZC, Li Q, Chen GN (2007) Fast colorimetric detection of copper ions using L-cysteine functionalized gold nanoparticles. J Nanosci Nanotechnol 7(2):712–716